4Lor2D-02

Magnetization in ReBCO-based CORC Cables in Magnetic Fields up to 30 T for Accelerator Applications

T. Garg, J. Jaroszynski, E.S. Choi, M.D. Sumption, M. Majoros, and E.W. Collings

***Abstract*—This study presents experimental measurements of the magnetization of ReBCO CORC cables in magnetic fields up to 30 T at 4.2 K. Such data are relevant for accelerator, fusion, and other potential applications. The cable was comprised of 29 ReBCO tapes, with a cable OD of 3.63 mm and cable pitch of 7.16 mm. The tapes were 2 mm wide, had a substrate thickness of 30 µm, and a Cu plating thickness of 5 µm. The cable had an I_c of 1675 A at 77 K and self-field. The CORC cable was received from Lawrence Berkeley National Laboratory (LBNL) with ID 170131-Berkeley. We used a susceptibility technique, with the NHMFL's Bitter (resistive) magnet acting as the primary coil. We constructed a sample holder with a pick-up coil (secondary) as well as a compensation coil. The CORC cables were measured first as a single and then a three-stack CORC, placed with the field perpendicular to the conductor length. Magnetization (M) versus applied magnetic field ($\mu_0 H$) was measured for field sweeps with amplitudes up to ± 30 T. Additionally, "accelerator-like" magnetic cycles were performed. Here, the field, initially at some low (1 T) "injection" field was increased to the maximum ("collision") field, ramped back to some hold field near zero (B_h), and then increased to the nominal injection field again, mimicking operational conditions relevant to particle accelerators. The magnetization at injection (taken here as 1 T) was observed to be ≅ 1100 kA/m. Furthermore, the penetration field (B_p), which defines the point at which flux reaches the center of the conductor, was found to increase from 1.2 to 2 T when we moved from a single-stack to a three-stack of cables. These measurements are important for understanding the CORC cable's implementation in high-field applications such as particle accelerators.**

***Index Terms*— CORC, HTS, Magnetization, and ReBCO.**

I. Introduction

SUPERCONDUCTING cables, such as Rare-earth Barium Copper Oxide (ReBCO) Conductor on Round Core (CORC), are critical, enabling components of high-field magnets for the next generation of particle accelerators [1], [2], fusion reactors [3-5], and other advanced applications. These cables, which utilize high-temperature superconducting (HTS) materials, offer high current-carrying capacities and have exciting potential for these applications because of their large upper critical fields and excellent high-field transport properties [6-8]. However, the presence of magnetization effects poses significant challenges to their practical implementation, affecting the beam steering accuracy as well as the efficiency and stability of the systems they are employed in.

As one example, we can consider a superconducting dipole magnet used for particle beam steering. For optimal steering, these should have a pure dipole field. However, such magnets will have multipolar distortion if the conductors have magnetization. Shielding or trapping currents within the wires generate this magnetization, and the resulting field errors depend on both the superconducting strand and cable properties and the overall coil particulars [9-11].

Previous studies have provided insights into the mechanisms of flux penetration and magnetization in CORC cables, particularly at the injection fields of accelerator magnets [12],[13]. Furthermore, modification of magnetization properties through pre-injection cycles has previously been explored, demonstrating the potential for optimizing cable performance [14]. *M-H* measurements for ReBCO tapes can, at least at some level, be performed using a PPMS or MPMS (SQUID) system, but such systems cannot be used for ReBCO cables because of sample size restrictions in these devices (typically, samples must be 5 mm or less in all dimensions). Such cables have been measured using a Hall probe technique with the applied field provided by a liquid cryogen-free, 12 T magnet located here at OSU [14], [15]. Some high field torque magnetometer measurements have been made on single tapes [16]. Our group has also used a susceptibility technique employing a ± 3 T superconducting dipole magnet in combination with a pickup and compensation coil to study the magnetization of ReBCO based Roebel and CORC cables [12]. However, the nominal design fields for ReBCO based high field magnet dipole inserts are in the 20 T range, and it is thus important to study the *M-H* behavior of these cables at higher fields. Other applications, e.g., fusion, are also impacted by the high field properties of these conductors. As will be seen below, it is also important to measure not only cables but stacks of cables to better understand the expected magnetization and penetration fields of these cables and cable stacks and their

This work was supported in part by the United States Department of Energy, Office of Science, Division of High Energy Physics under Grant DE-SC0011721. *(Corresponding author: T. Garg).*

A portion of this work was performed at the National High Magnetic Field Laboratory, which is supported by National Science Foundation Cooperative Agreement No. DMR-2128556 and the State of Florida.

T. Garg, M.D. Sumption, M. Majoros, and E.W. Collings are with the Center for Superconducting and Magnetic Materials, Materials Science Department, Ohio State University, Columbus, OH 43210 USA (e-mail: garg.206@ osu.edu).

J. Jaroszynski, and E.S. Choi are with Applied Superconductivity Center, National High Magnetic Field Laboratory, Tallahassee, Florida, 32310, USA.

impact on magnet performance. For this reason, we have developed an approach to measure the conductor properties up to 30 T in the resistive magnets of the NHMFL.

II. Experimental

A. Samples

All samples measured in this work were cut from a CORC cable made up of 29 ReBCO tapes, cable OD 3.63 mm, and with a cable pitch of 7.16 mm. The ReBCO tapes were 2 mm wide and had a substrate thickness of 30 µm and a Cu plating thickness of 5 µm. The cable I_c was 1675 A at 77 K and self-field [17]. The CORC cable was received from Lawrence Berkeley National Laboratory (LBNL) with ID 170131-Berkeley. Two samples were measured; the first consisted of a single CORC cable 2.7 cm long (the single CORC sample), and the second sample had three 2.7 cm long segments of the cable. We used a diamond saw to cut the samples. In all cases, the field was perpendicular to the conductor length, and for the three-stack cable, the wide dimension of the cable stack was along the field direction, as shown in Fig. 1.

The single-stack CORC was measured first. Measurements on these samples were made with a magnetic field orthogonal to the cable's longitudinal axis in a LHe environment (4.2 K), using distinctive field cycles. The specifications of these CORC cables are listed in Table I, see also [17].

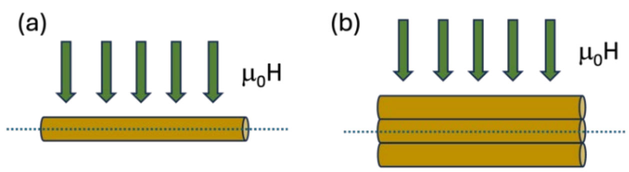

Fig. 1. Schematic of the applied field to the (a) single CORC and (b) three-stack CORC. The yellow cylinders are the CORC, and the arrows represent the applied field.

TABLE I
CORC Sample Details

Cable diameter	3.63 mm
Diameter of Cu core	2.56 mm
Number of tapes	29
Tape width	2 mm
Cu plating thickness	5 µm
Substrate thickness	30 µm
Cross sectional area	10.35 mm^2
Percentage of Cu area	55 %
Cable pitch	7.16 mm
Sample length	27 mm
n-value @77K and self-Field	31.6
Critical Current @77K and self-Field, I_c	1675 A

B. Pickup Coil Development

Fig. 2 shows a CAD drawing for the parts and an assembly drawing of the pick-up coil including (a) the top part that connects to the probe, (b) the bottom bit that presses on the sample keeping it in place, (c) the support rods, (d) the central region, containing the pick-up and compensation coils, and (e) the fully assembled sample holder. Fig. 3 shows the as-fabricated components, including (a) top, (b) bottom, (c) support rods, (d) pickup and compensation coils, (e) full assembly, and (f) full sample rod with sample holder at the right end (bottom of probe). The sample holder was made from G10, and the pickup and compensation coils were wound with Cu AWG-34 Polyurethane/Nylon coated wire. Each coil consisted of 7 layers of windings, and each layer had ~165 turns. Further pickup coil specifications are listed in Table II.

TABLE II
Pick-up Coil Specifications

Shape	Square cylinder type
Dimensions	32.5 × 30 × 8 mm
Number of turns per layer	~165
Number of layers	7
Wire material	Cu with PUR/Nylon insulation
Wire diameter	0.18 mm (AWG-34)

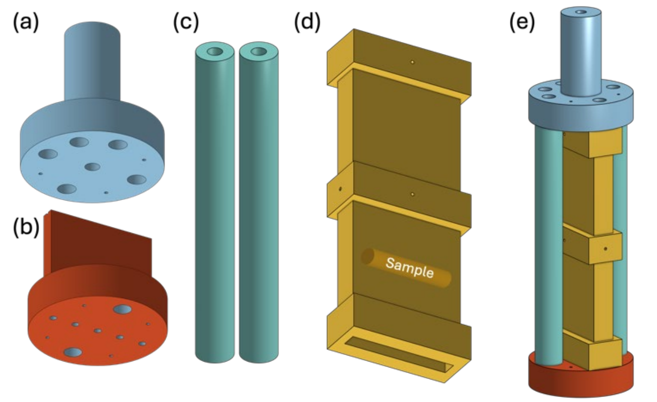

Fig. 2. Pick-up coil CAD drawing: (a) the top part that connects to the probe, (b) the bottom bit that presses on the sample, keeping it in place, (c) the support rods, (d) the central region with the sample, containing the pick-up and compensation coils, and (e) the fully assembled sample holder.

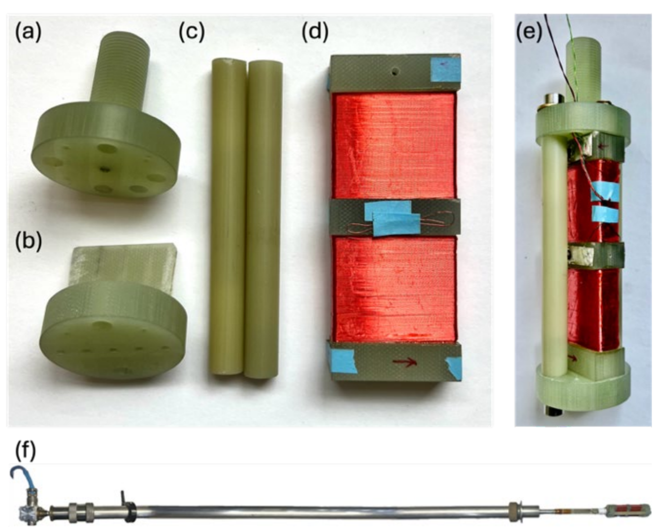

Fig. 3. Machined Pick-up coil with windings, including (a) top, (b) bottom, (c) support rods, (d) pickup and compensation coils, (e) full assembly, and (f) full sample rod with sample holder at the right end (bottom of probe).

C. Measurement Procedure

We utilized a Florida Bitter Magnet as the primary field source and a custom coil set from OSU for both the pickup and

This article has been accepted for publication in IEEE Transactions on Applied Superconductivity. This is the author's version which has not been fully edited and content may change prior to final publication. Citation information: DOI 10.1109/TASC.2025.3540991

compensation coils. Magnetic fields were induced in the secondary coil by ramping the field produced by the Bitter Magnet. The induced voltage, *V,* in the coil, can be calculated using Faraday's law. In principle, a compensation coil, connected to the pickup coil in an anti-series configuration, nullifies the induced voltage signal in the absence of a sample. In practice, imperfect matching of the pickup and compensation coil are corrected by using a voltage divider network to select some fraction of the compensation coil voltage. The use of a variable resistor in this circuit allows us to carefully adjust the system so that the cancellation is optimized with no sample in the sample coil. Then when a sample is placed in the secondary coil, it disrupts the balance, causing a resultant voltage which can be integrated over time to determine the flux. This flux is then calibrated to get the magnetization, *M*, of the sample. In our case, calibration was achieved by measuring flux exclusion on the Meissner slope of the initial magnetization curve, assuming a cylindrical sample with a demagnetization factor of 1/2. This procedure has been validated for a CORC sample in Ref [14], [15].

III. Results

A. M-H loops

Our first *M-H* measurements were performed on the single-stack CORC cable (at 4.2 K) using a field sweep of ± 10 T. A ramp rate of 10 T/min was used for these measurements. The results, with magnetization normalized to cable volume, are shown in Fig 4. This single-CORC shows a penetration field, B_p, of 1.2 T and a magnetization corresponding to full flux penetration, M_p, of 1300 kA/m. Some drift is observed in the magnetization signal, which prevents overlap of the initial and final branches.

Fig. 5 shows the magnetization measurements for a three-stack of CORC cables with a maximum field sweep of ± 30 T. To our knowledge, this represents the first measurement of *M-H* for a CORC cable out to such fields and we expect that these results are of significant interest to the particle accelerator magnet community, as well as the fusion community. We performed a few sweep cycles starting from ± 10 T and incrementing by 5 T up to ± 30 T. We observed an increase in B_p for the three-stack CORC as compared to the single CORC. The three-stack CORC shows a B_p = 2 T and a magnetization above penetration, M_p, of 1300 kA/m. Some small baseline curvature is seen for the *M-H* at highest fields, the origin of this is unclear.

B. Accelerator Cycle

Next, the *M-H* response of the CORC cable sample was studied by means of a series of steps that imitate the operational field cycling of a particle accelerator. The purpose of this experiment was to observe the magnetization at the injection field and how it changes with different accelerator field cycles

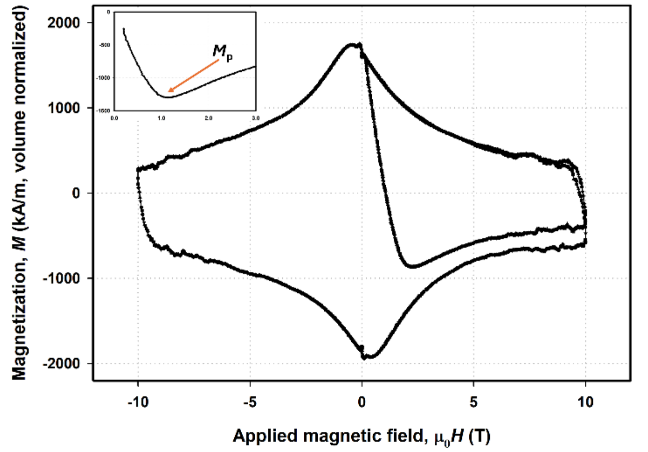

Fig. 4. The measured *M-H* hysteresis loop at 4.2 K of a single CORC sample, subjected to a maximum field of 10 T, applied orthogonal to the cable's longitudinal axis.

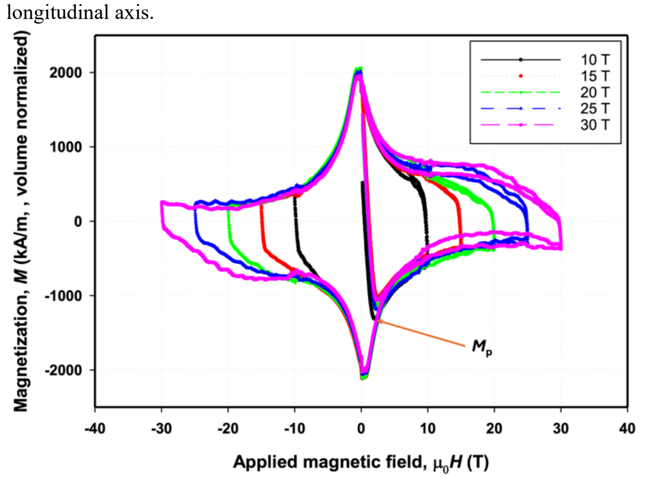

Fig. 5. The measured *M-H* hysteresis loop at 4.2 K of a three-stack CORC stack sample, subjected to a maximum field of 30 T, applied orthogonal to the cable's longitudinal axis.

and low field "hold" values. The sequence involved: (1) ramping the magnetic field from 0 T to a peak field of from 9 T-20 T, well above the injection field. (2) The field was then reduced to a lower "hold" field (B_h), below the injection field, (0-1 T). (3) Finally, the field was ramped back up to the injection field, set at 1 T in this case. Different hold fields of 0, 0.2, 0.4, 0.6, 0.8, and 1 T were tested during the experiment. These steps allowed for the evaluation of the magnetization and its behavior as a function of the field cycle protocol. The overall goal was to see what cycles led to the lowest magnetization at injection, and how this would change for different cable stackings. The outcomes of the accelerator like cycle measurements are illustrated in Figures 6 and 7.

Fig. 6 shows the accelerator cycles for the single CORC sample with different hold fields of 0, 0.2, 0.4, 0.6, 0.8, and 1 T. These accelerator cycles were performed with the maximum field of 9 T. Fig. 7 shows the accelerator cycles for the three-stack CORC sample with different hold fields of 0, 0.2, 0.4, 0.6, 0.8, and 1 T and ramping up to a field of 20 T.

This article has been accepted for publication in IEEE Transactions on Applied Superconductivity. This is the author's version which has not been fully edited and content may change prior to final publication. Citation information: DOI 10.1109/TASC.2025.3540991

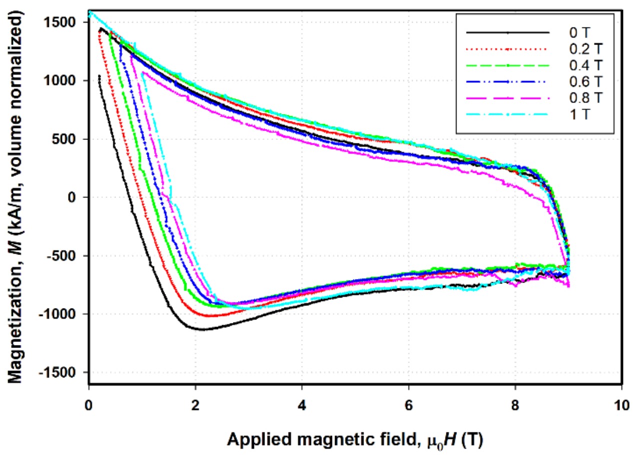

Fig. 6. Accelerator like *M-H* cycle measured at different hold fields of 0, 0.2, 0.4, 0.6, 0.8, 1 T for single CORC sample, replicating the field cycling sequence of acceleration, collision, beam dump, and reinjection.

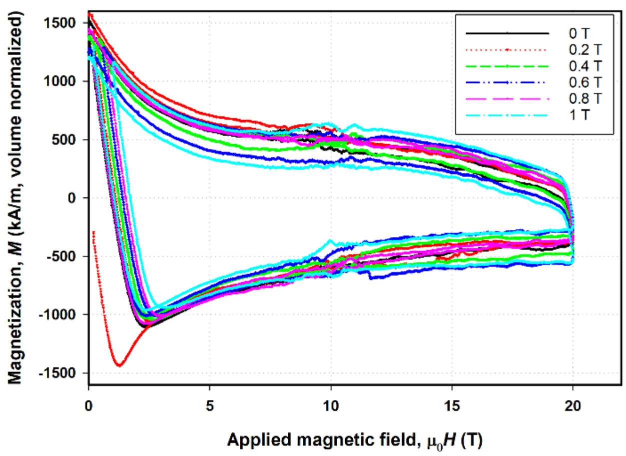

Fig. 7. Accelerator like *M-H* cycle measured at different hold fields of 0, 0.2, 0.4, 0.6, 0.8, 1 T for three-stack CORC sample, replicating the field cycling sequence of acceleration, collision, beam dump, and reinjection.

C. Changes in B_p and M at Injection

We evaluated the magnetization at the injection field (1 T) for both single and three-stack CORC cables under various hold fields, as shown in Fig. 8. The magnetization above penetration was essentially the same for the single CORC to the three- stack configuration. This is as expected, since in this regime, the magnetization per unit volume is just proportional to the flux excluded by the shielding (or trapping) currents, i.e., $\propto J_c\, d_{eff}$, where d_{eff} is the length scale of the field gradient in the sample (the same for single or stacked cables). Magnetization in fact peaks at M_p (which occurs at B_p) since $\underline{J_c}$ drops with increasing field. On the other hand, the penetration field (B_p) for the single CORC was 1.2 T, while for the three-stack CORC it increased to 2 T, marking a 60% rise due to stacking. This result is not very surprising, since it is known that stacking ReBCO conductors can increase the field at which flux penetration is achieved, and modifying loss and *M-H* in low field regimes [18-21], although we are unaware of its previous demonstration in stacks of CORC cables.

To minimize magnetization at injection in accelerator magnets, it is essential to find a field cycle that reduces magnetization as much as possible. The magnetization can remain too high if the field only cycles between injection and collision values. By ramping down to zero or a low hold field before returning to injection, the magnetization is reduced, minimizing field distortions. The magnetization at 1 T after cycling to high field, down to B_h, and then to 1 T, is different for the single CORC and the 3-stack because in this case $B_h < B_p$, thus we are in the low field regime at 1 T, and M at 1 T increases as B_p-B_h decreases (i.e., M_p occurs at B_p). In our case, Fig. 8 shows that to minimize magnetization to near zero, a B_h value of 0.2 T is required for a single CORC while a B_h of 0.1 T is required for a three-stack CORC. The process may vary depending on the cable's structure, such as single versus multi-stack CORC. Indeed, for an actual magnet or magnet insert, it will be difficult to completely remove the magnetization (and associated field errors) because different portions of the winding will experience different fields at the same bore field (e.g., at injection). In any case, detailed studies and adjustment for different configurations will be required to optimize performance.

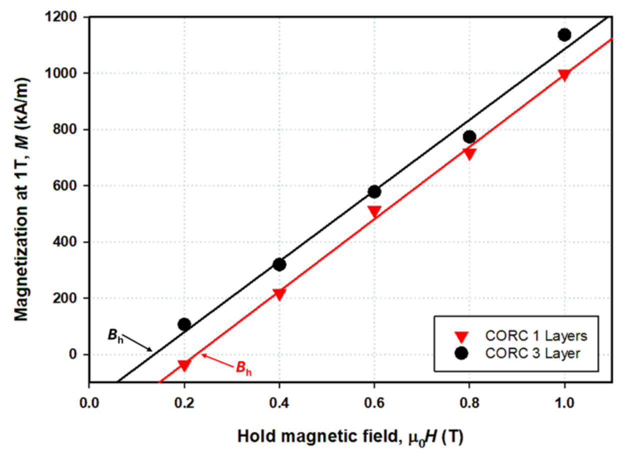

Fig. 8. Magnetization at the hold field, B_h, for accelerator cycles. These values of B_h can be compared to the 1 T nominal "injection field" at which the *y*-axis magnetization is measured, as well as B_p (1.2 T for the 1 stack CORC sample, and 2 T for the 3 stack CORC sample).

IV. Conclusion

We measured *M-H* loops for CORC cables at fields up to 30 T, utilizing a Bitter magnet as the primary and custom-developed secondary and compensation coils. Our analysis focused on accelerator injection cycles using CORC and stacked CORC, where the penetration field varied with stacking, altering the magnetization at injection. The penetration field, B_p, for the single CORC, was 1.2 T while the penetration field, B_p, for the three-stack CORC was 2 T, which is a 60% increase due to stacking. The magnetization correlating to the penetration field, M_p, was 1300 kA/m for both samples.

Magnetization in accelerator magnets is minimized by cycling the field to zero or a low hold value, reducing distortions. Notably, our results show that to minimize the magnetization to near zero the single CORC exhibits a hold field, B_h value approaching 0.2 T, whereas the three-stack CORC stack achieves a significantly lower B_h of approximately 0.1 T. We see that we can expect that the choice of ramping protocol to minimize magnetization at a given field (e.g. injection) depends on cable configuration, with single and multi-stack CORC stacks requiring tailored approaches. The results provide valuable insights for high-energy physics (HEP) dipole magnet applications and may also be of interest for fusion magnet applications.

REFERENCES

[1] L. Bottura, S. A. Gourlay, A. Yamamoto, and A. V. Zlobin, “Superconducting Magnets for Particle Accelerators,” *IEEE Transactions on Nuclear Science*, vol. 63, no. 2, pp. 751–776, Apr. 2016, doi: 10.1109/TNS.2015.2485159.

[2] L. Rossi and C. Senatore, “HTS Accelerator Magnet and Conductor Development in Europe,” *Instruments*, vol. 5, no. 1, Art. no. 8, Mar. 2021, doi: 10.3390/instruments5010008.

[3] N. Mitchell *et al.*, “Superconductors for fusion: A roadmap,” *Supercond Sci Tech*. vol. 34, no. 10, pp. 57, Sep. 2021, Art no. 103001, doi: 10.1088/1361-6668/ac0992.

[4] P. Bruzzone *et al.*, “High temperature superconductors for fusion magnets,” *Nucl. Fusion*, vol. 58, no. 10, pp. 13, Aug. 2018, Art no. 103001, doi: 10.1088/1741-4326/aad835.

[5] W. H. Fietz *et al.*, “Prospects of High Temperature Superconductors for fusion magnets and power applications,” *Fusion Engineering and Design*, vol. 88, no. 6, pp. 440–445, Oct. 2013, doi: 10.1016/j.fusengdes.2013.03.059.

[6] S. Hahn *et al.*, “45.5-tesla direct-current magnetic field generated with a high-temperature superconducting magnet,” *Nature*, vol. 570, no. 7762, pp. 496–499, Jun. 2019, doi: 10.1038/s41586-019-1293-1.

[7] J. Liu, Q. Wang, L. Qin, B. Zhou, K.Wang, Y. Wang, L. Wang, Z. Zhang, Y. Dai, H. Liu, et al, “World record 32.35 tesla direct-current magnetic field generated with an all-superconducting magnet”, *Supercond. Sci. Technol*. 33 (2020) 03LT01 DOI 10.1088/1361-6668/ab714e

[8] R. Gupta *et al.*, “Hybrid High-Field Cosine-Theta Accelerator Magnet R&D With Second-Generation HTS,” *IEEE Trans Appl. Supercon*, vol. 25, no. 3, pp. 1–4, Jun. 2015, Art no. 4003704, doi: 10.1109/TASC.2014.2364400.

[9] M. Majoros, M. D. Sumption, S. Xue, C. S. Myers, and E. W. Collings, “A Field Quality Modeling in Canted Cosine Theta Dipole Magnets Wound Using ReBCO Cables,” *IEEE Trans. Appl. Supercon,* vol. 34, no. 5, pp. 1–4, Aug. 2024, Art no. 4903404, doi: 10.1109/TASC.2024.3365092.

[10] M. Majoros, M. D. Sumption, C. S. Myers, and E. W. Collings, “Canted Cosine Theta Dipole Magnet Wound Using ReBCO CORC Cables–The Effect of Magnetization on Magnetic Field Quality,” *IEEE Transactions on Applied Superconductivity*, vol. 33, no. 5, pp. 1–5, Aug. 2023, Art no. 4003705, doi: 10.110 *IEEE Trans. Appl. Supercon,* 9/TASC.2023.3265574.

[11] L. Bortot *et al.*, “High-temperature superconducting screens for magnetic field-error cancellation in accelerator magnets,” *Supercond. Sci. Technol.*, vol. 34, no. 10, pp. 15, Aug. 2021, Art no. 105001, doi: 10.1088/1361-6668/ac1c13.

[12] C. Kovacs, M. Majoros, M. D. Sumption, and E. W. Collings, “Magnetization Measurements of CORCTM and Roebel Type YBCO Cables for Accelerators Using a ±3-T Dipole Magnetometer,” *IEEE Trans. Appl. Supercon*, vol. 29, no. 5, pp. 1–5, Aug. 2019, Apt no. 8200905, doi: 10.1109/TASC.2019.2898254.

[13] M. D. Sumption *et al.*, “AC losses of Roebel and CORC® cables at higher AC magnetic fields and ramp rates,” *Supercond. Sci. Technol.*, vol. 35, no. 2, pp. 10, Dec. 2021, Art no. 025006, doi: 10.1088/1361-6668/ac3b62.

[14] C. S. Myers, M. D. Sumption, and E. W. Collings, “Magnetization and Flux Penetration of YBCO CORC Cable Segments at the Injection Fields of Accelerator Magnets,” *IEEE Trans. Appl. Supercon,* , vol. 29, no. 5, pp. 1–5, Aug. 2019, Art no. 4701105, doi: 10.1109/TASC.2019.2896625.

[15] C. S. Myers, M. D. Sumption, and E. W. Collings, “Magnetization and Creep in YBCO Tape and CORC Cables for Particle Accelerators: Value and Modification Via Preinjection Cycle,” *IEEE Trans. Appl. Supercon,* , vol. 29, no. 5, pp. 1–5, Aug. 2019, Art no. 8201405, doi: 10.1109/TASC.2019.2898119.

[16] J. Jaroszynski, “Application of Torque Magnetometry for 2G HTS Characterization up to 45 T,” presented at the EUCAS, manuscript to be submitted.

[17] X. Wang *et al.*, “A viable dipole magnet concept with ReBCO CORC® wires and further development needs for high-field magnet applications,” *Supercond. Sci. Technol.*, vol. 31, no. 4, pp. 10, Mar. 2018, Art no. 045007, doi: 10.1088/1361-6668/aaad8f.

[18] M. D. Sumption, C. Ebbing, G. Panasyuk, C. Kovacs, G. J. P. Murphy et al., “AC loss and shielding in stacks of coated conductors: Analytic modelling and comparison to experiment,” *Cryogenics*, vol. 144, p. 103963, Dec. 2024, doi: 10.1016/j.cryogenics.2024.103963.

[19] S. Matsumoto, T. Kiyoshi, and A. Uchida, “Shielding of Magnetic Fields by REBCO Coated Conductors,” *IEEE Trans. Appl. Supercond.*, vol. 21, no. 3, pp. 2283–2286, Jun. 2011, doi: 10.1109/TASC.2010.2089036.

[20] ter Harmsel J, Otten S, Dhall´e M, ten Kate H. “Magnetization loss and transport current loss in ReBCO racetrack coils carrying stationary current in time-varying magnetic field at 4.2 K,” *Supercond. Sci. Technol.,vol.* 36, pp. 11, Dec. 2023, Art no. 015011, doi: 10.1088/1361-6668/aca83d.

[21] Pardo E, Souc J, Kovac J. “AC loss in REBCO pancake coils and stacks of them: modeling and measurement,” *Supercond. Sci. Technol., vol.* 25, pp. 16, Jan. 2012, Art no. 035003, doi: 10.1088/0953-2048/25/3/035003.